Mem. S.A.It. Vol. 74, 942

Memorie della

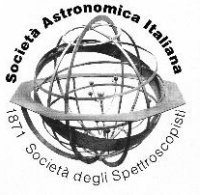

The physics and astrophysics of type Ia supernova explosions

W. Hillebrandt[1], J.C. Niemeyer[1], M. Reinecke[1] and C. Travaglio[1]

Max-Planck-Institut für Astrophysik, Karl-Schwarzschild-Str. 1, D-85741 Garching, Germany e-mail: wfh@mpa-garching.mpg.de

Abstract. Because calibrated light curves of type Ia supernovae have become a major tool to determine the local expansion rate of the Universe, considerable attention has been given to models of these events over the past couple of years. Recent progress in modeling type Ia supernovae as well as several of the still open questions are addressed in this article. Although the main emphasis will be on studies of the explosion mechanism itself and on the related physical processes, including the physics of turbulent nuclear combustion in degenerate stars, observational implications and constraints will also be discussed.

Key words. Abundances – Hydrodynamics – Nucleosynthesis – Supernovae

1. Introduction

Type Ia supernovae are stellar explosions which show no signs of hydrogen in their spectra but intermediate mass elements such as Si, S, Ca, and Mg near maximum light, and many lines of Fe at late times. They also show no He. The most popular progenitor model for the average type Ia supernovae, therefore, is a massive white dwarf, consisting of carbon and oxygen, which approaches the Chandrasekhar mass $M_{\rm Chan}$ by a yet unknown mechanism, presumably accretion from a companion star, and is disrupted by a thermonuclear explosion (see, e.g., Hillebrandt & Niemeyer (2000) for a recent review). A second argument in favor of this hypothesis is the ability of these explosion models to fit the observed light curves and spectra well (Leibundgut 2001).

Modeling a type Ia supernova explosion, therefore, means that we have to compute the thermonuclear disruption of a white dwarf. However, the evolution of massive white dwarfs to explosion is very uncertain, leaving room for some diversity in the allowed set of initial conditions (such as the temperature profile at ignition), and also the physics of thermonuclear burning in degenerate matter is complex and not well understood. In the generally accepted scenario explosive carbon burning is ignited either at the center of the star or off-center in a couple of ignition spots, depending on the details of the previous evolution. After ignition, the flame is thought to propagate through the star as a sub-sonic deflagration wave which may or may not change

Send offprint requests to: W. Hillebrandt
Correspondence to: Karl-Schwarzschild-Str. 1, D-85741 Garching

into a detonation at low densities (around $10^7 \mathrm{g/cm}^3$). Numerical models with parameterized velocity of the burning front have been very successful, the prototype being the W7 model of Nomoto et al. (Nomoto, Thielemann & Yokoi 1984).

Unfortunately these models did not solve the problem because all attempts to determine the effective flame velocity from direct numerical simulations failed and gave velocities far too low for successful explosions (Khokhlov 1995; Arnett & Livne 1994). However, there is a way out of this dilemma. Shear-induced turbulence at the interface between burned and unburned gas should play a major role, because turbulence increases the effective surface area of the flamelets and, thereby, the rate of fuel consumption. Of course, 1D simulations could not model this.

Here, we present 2D and 3D simulations which demonstrate that this idea, in principle, does work. It is very encouraging that all our models predict explosions, with energies in the range of observed type Ia supernovae, and that these models predict also light curves which fit the observations very well. In addition, also their nucleosynthesis products are in reasonable agreement with expectations.

2. Turbulent thermonuclear burning in degenerate C+O matter

Due to the strong temperature dependence of the C-fusion reaction rates nuclear burning during the explosion is confined to microscopically thin layers that propagate either conductively as subsonic deflagrations ("flames") or by shock compression as supersonic detonations (Landau & Lifshitz 1995). Both modes are hydrodynamically unstable to spatial perturbations as can be shown by linear perturbation analysis. In the nonlinear regime, the burning fronts are either stabilized by forming a cellular structure or become fully turbulent – either way, the total burning rate increases as a result of flame surface growth. Neither flames nor detonations can be resolved in explosion simulations on stellar scales and therefore have to be represented by numerical models.

The best studied and probably most important hydrodynamical effect for modeling SN Ia explosions is the Rayleigh-Taylor (RT) instability resulting from the buoyancy of hot, burned fluid with respect to the dense, unburned material (Müller & Arnett 1982; Niemeyer & Hillebrandt 1995), and after more than five decades of experimental and numerical work, the basic phenomenology of nonlinear RT mixing is fairly well understood.

Secondary instabilities related to the velocity shear along the bubble surfaces (Niemeyer & Hillebrandt 1995) quickly lead to the production of turbulent velocity fluctuations that cascade from the size of the largest bubbles ($\approx 10^7$ cm) down to the microscopic Kolmogorov scale ($\approx 10^{-3}$ cm) where they are dissipated. Since no computer is capable of resolving this range of scales, one has to resort to statistical or scaling approximations of those length scales that are not properly resolved. The most prominent scaling relation in turbulence research is Kolmogorov's law for the cascade of velocity fluctuations, stating that in the case of isotropy and statistical stationarity, the mean velocity v of turbulent eddies with size l scales as $v \sim l^{1/3}$ (Kolmogorov 1941).

Given the velocity of large eddies, e.g. from computer simulations, one can use this relation to extrapolate the eddy velocity distribution down to smaller scales under the assumption of isotropic, fully developed turbulence. Turbulence wrinkles and deforms the flame. These wrinkles increase the flame surface area and therefore the total energy generation rate of the turbulent front. In other words, the turbulent flame speed, S_t, defined as the mean overall propagation velocity of the turbulent flame front, becomes larger than the laminar speed S_l. If the turbulence is sufficiently strong, $v(L) \gg S_\mathrm{l}$, the turbulent flame speed becomes independent of the laminar speed, and therefore of the microphysics of

burning and diffusion, and scales only with the velocity of the largest turbulent eddy (Clavin 1994).

As the density of the white dwarf material declines and the laminar flamelets become slower and thicker, it is plausible that at some point turbulence significantly alters the thermal flame structure (Niemeyer & Woosley 1997). So far, modeling this so-called distributed burning regime in exploding white dwarfs has not been attempted explicitly since neither nuclear burning and diffusion nor turbulent mixing can be properly described by simplified prescriptions. However, it is this regime where the transition from deflagration to detonation is assumed to happen in certain phenomenological models.

3. Application to the supernova problem

Based on these ideas we have developed a numerical method to model turbulent thermonuclear combustion in degenerate white dwarfs. We have carried out numerical simulations in 2D and 3D, for a variety of different initial conditions, and for changing numerical resolution. Details of these models, including tests of numerical convergence, are given in a series of papers (Reinecke, Hillebrandt & Niemeyer 1999, 2002a,b). Therefore only some of the essential results are repeated here.

In all our simulations the white dwarf, constructed in hydrostatic equilibrium for a realistic equation of state, has a central density of $2.9{\cdot}10^9 \mathrm{g/cm^3}$, a radius of $1.5{\cdot}10^8 \mathrm{cm}$, and a mass of $2.8{\cdot}10^{33} \mathrm{g}$, identical to the one used in (Niemeyer & Hillebrandt 1995). The initial mass fractions of C and O are chosen to be equal, and the total binding energy is $5.4{\cdot}10^{50} \mathrm{erg}$. At low densities ($\rho \leq 10^7 \mathrm{g/cm^3}$), the burning velocity of the front is set equal to zero because the flame enters the distributed regime and our physical model is no longer valid. However, since in reality some matter may still burn the energy release obtained in the simulations is probably somewhat too low.

3.1. Numerical convergence and 2D versus 3D

The energy liberated by turbulent nuclear combustion in 2D models of different numerical resolution is given in Fig.1. It shows that once we use sufficient resolution, at least a 256^2 grid in this case, the global properties of the supernova model are only weakly dependent on resolution, indicating the validity of the "Large Eddy" approach. The reason is that the rate of fuel consumption, in first order, increases proportional to surface area of the burning front and better resolved flames have more surface. However, this effect is compensated by the fact that on smaller scales the velocities are lower. Since the fuel consumption rate is proportional to the product of flame surface and turbulent flame velocity, differently resolved both models predict similar explosion energies.

The same Figure also shows a comparison between two models with identical initial conditions (a flame ignited at the white dwarf's center with 3 "fingers"; see Reinecke, Hillebrandt & Niemeyer (2002a)) but going from axial symmetry to 3 spatial dimensions. In the beginning the evolution is rather similar in both cases. However, at later times 3D structures begin to grow, originally due to numerical noise, and destroy the symmetry. Consequently the surface area of the nuclear flame grows faster in 3D than in 2D with obvious impact on the final explosion energy.

3.2. The effect of different initial conditions

In our approach, the initial white dwarf model (composition, central density, and velocity structure), as well as assumptions about the location, size and shape of the flame surface as it first forms fully determine the simulation results. At present,

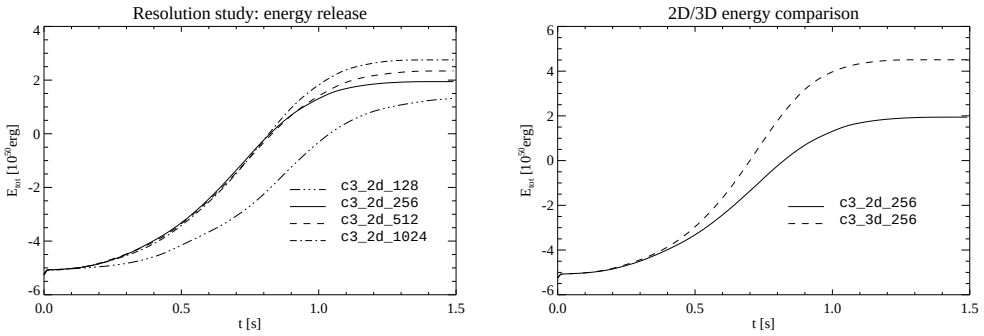

Fig. 1. Left panel: Nuclear energy generation for explosion models with different numerical resolution (from 128^2 through 1024^2). All models with a grid of at least 256^2 points have an almost identical energy generation rate for the first second of the explosion. Later deviations are caused by the distortion of the grid at large radii. Right panel: 2D versus 3D model. Since 3D structures possess a larger surface area per volume, for given initial conditions the explosion energy is higher in 3D.

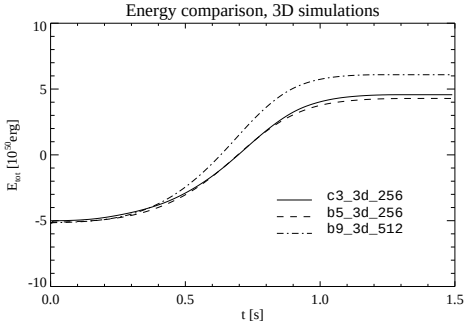

Fig. 2. Energy evolution of the off-center 3D explosion models discussed in the text (dashed and dashed-dotted). For comparison we also show the centrally ignited ("three fingers") model of Reinecke, Hillebrandt & Niemeyer (2002a) (solid line).

we have not changed the properties of the white dwarf but we concentrate on variations of the latter. In this context, the simultaneous runaway at several different spots in the central region of the progenitor star is of particular interest, a plausible ignition scenario suggested by Garcia-Senz & Woosley (1995).

One simulation was carried out on a grid of 256^3 cells with a central resolution of 10^6 cm and contained five bubbles with a radius of $3{\cdot}10^6$ cm, which were distributed randomly in the simulated octant within $1.6{\cdot}10^7$ cm of the star's center. In an attempt to reduce the initially burned mass as much as possible without sacrificing too much flame surface, a very highly resolved second model was constructed. It contains nine randomly distributed, non-overlapping bubbles with a radius of $2{\cdot}10^6$ cm within $1.6{\cdot}10^7$ cm of the white dwarf's center. To properly represent these very small bubbles, the cell size was reduced to $\Delta = 5{\cdot}10^5$ cm, so that a total grid size of 512^3 cells was required.

During the first 0.5 seconds, the three models are nearly indistinguishable as far as the total energy is concerned (see Fig. 2), which at first glance appears somewhat surprising, given the quite different initial conditions. A closer look at the energy generation rate actually reveals noticeable differences in the intensity of thermonuclear burning for the simulations, but since the total flame surface is initially very small, these differences have no visible impact on the integrated curve in the early stages.

However, after about 0.5 seconds, when fast energy generation sets in, the nine-bubble model burns more vigorously due

to its larger surface and therefore reaches a higher final energy level. Fig. 2 also shows that the centrally ignited model (c3_3d_256) is almost identical to the off-center model b5_3d_256 with regard to the explosion energetics. But, obviously, the scatter in the final energies due to different initial conditions appears to be small. Moreover, all models explode with an explosion energy in the range of what is observed.

4. Predictions for observable quantities

In this Section we present a few preliminary results for various quantities which could, in principle, be observed and which therefore can serve as tests for the models.

4.1. Lightcurves

The most direct test of explosion models is provided by observed lightcurves and spectra. According to "Arnett's Law" lightcurves measure mostly the amount and spatial distribution of radioactive ^{56}Ni in type Ia supernovae, and spectra measure the chemical composition in real and velocity space.

Sorokina & Blinnikov (2002) have used the results of our centrally ignited 3D-model, averaged over spherical shells, to compute colour lightcurves in the UBVI-bands. Their code assumes LTE radiation transport and loses reliability at later times (about 4 weeks after maximum) when the supernova enters the nebular phase. Also, this assumption and the fact that the opacity is not well determined at longer wavelength make I-lightcurves less accurate. Keeping this in mind, the lightcurves shown in Fig. 3 look very promising. The main reason for the good agreement between the model and SN 1994D is the presence of radioactive Ni in outer layers of the supernova model at high velocities which is not predicted by spherical models.

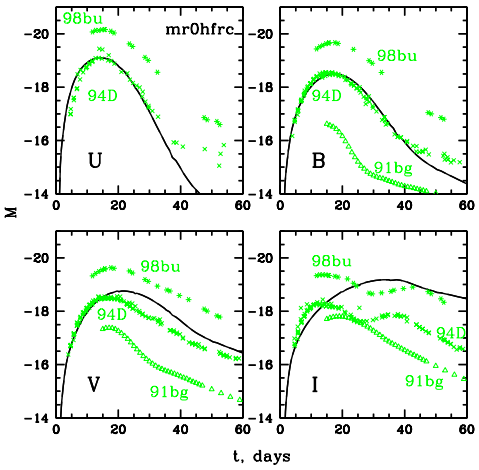

Fig. 3. UBVI-colour lightcurves predicted by a centrally ignited 3D model (solid lines) in comparison with observed data for a bright (98bu), a "normal" (94D), and a subluminous (91bg) supernova.

4.2. Elemental and isotopic abundances

A summary of the abundances obtained for all 3D models is given in Table 1. Here "Mg" (as in Fig. 3) stands for intermediate-mass nuclei, and "Ni" for the iron-group. In addition, the total energy liberated by nuclear burning is given. Since the binding energy of the white dwarf was about $5{\cdot}10^{50}$ erg, all models do explode. Typically one expects that around 80% of iron-group nuclei are originally present as ^{56}Ni bringing our results well into the range of observed Ni-masses. This success of the models was obtained without introducing any non-physical parameters, but just on the basis of a physical and numerical model of subsonic turbulent combustion. We also stress that our models give clear evidence that the often postulated deflagration-detonation transition is not needed to produce sufficiently powerful explosions.

Finally, we have "post-processed" one of our 3D models in order to see whether or not also reasonable isotopic abundances are

Table 1. Overview over element production and energy release of all discussed supernova simulations. The energy is given in units of 10^{50} erg.

Model	$m_{\rm Mg}$ $[M_\odot]$	$m_{\rm Ni}$ $[M_\odot]$	$E_{\rm nuc}$
c3_3d_256	0.177	0.526	9.76
b5_3d_256	0.180	0.506	9.47
b9_3d_512	0.190	0.616	11.26

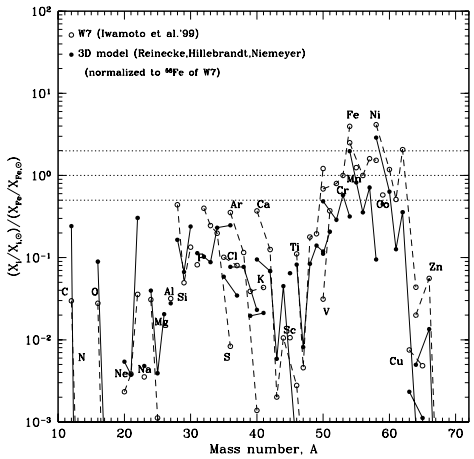

Fig. 4. Isotopic abundances (relative to solar) obtained for an off-center ignited 3D model. For comparison we show W7-nucleosynthesis predictions also.

obtained. The results, shown in Fig. 4, are very preliminary and should be considered with care. However, it is obvious that, with a few exceptions, also isotopic abundances are within the expected range. Exceptions include the high abundance of (unburned) C and O, and the overproduction of ^{54}Fe and ^{58}Ni. We think that this reflects a deficiency of the model, which burns some C and O at densities too high and temperatures too low. One may speculate that a bit lower ignition density would cure this problem.

5. Conclusions

In this article, we have discussed the physics of thermonuclear combustion in degenerate dense matter of C+O white dwarfs and have presented the first results of simulations of thermonuclear supernova explosions of $M_{\rm Chan}$ white dwarfs in 2 and 3 dimensions. All models we have computed (differing only in the ignition conditions and the grid resolution) explode. The explosion energy and the Ni-masses are only moderately dependent on the way the nuclear flame is ignited making the explosions robust. However, since ignition is a stochastic process, the differences we find may even explain some of the spread in observed SN Ia's.

Based on our models we can predict lightcurves, spectra, and abundances, and the first preliminary results look very promising. The lightcurves seem to be in excellent agreement with observations, and also the nuclear abundances of elements and their isotopes are found to be in the expected range. Therefore, it seems possible to link the models to observed explosions, thereby disentangling their physics. Of course, the next step is to compute a grid of models, with varying white dwarf properties, and to compare them with the increasing data base of well-observed type Ia supernovae. Here, in particular, it would be important to have photometric and spectroscopic data in all wave bands during all epochs, and early detections of type Ia supernovae by means of wide field imaging could be extremely valuable.

Acknowledgements. This work was supported by the *Deutsche Forschungsgemeinschaft, DFG* through the SFB 375 and project Hi 534/3.

References

W. D. Arnett, W. D. & Livne, E. 1994, ApJ 427, 31
Clavin, P. 1994, Ann. Rev. Fluid Mech. 26, 321
Garcia-Senz, D. & Woosley, S. E. 1995, ApJ 454, 895
Hillebrandt, W. & Niemeyer, J. C. 2000, Ann. Rev. Astron. Astrophys 38, 191
Khokhlov, A. M. 1995, ApJ 449, 695
Kolmogorov, A. N. 1941, Dokl. Akad. Nauk SSSR 30, 299
Landau, L. D. & Lifshitz, E. M. 1995, Fluid Mechanics, Butterworth-Heinemann
Leibundgut, B. 2001, Ann. Rev. Astron. Astrophys. 39, 67
Müller, E. & Arnett, W. D. 1982, ApJL 261, L109
Niemeyer, J. C. & Hillebrandt, W. 1995, ApJ 452, 769
Niemeyer, J.-C. & Woosley, S. E. 1997, ApJ 475, 740
Nomoto, K., Thielemann, F.-K. & Yokoi, K. 1984, ApJ 286, 644
Reinecke, M., Hillebrandt, W. & Niemeyer, J.-C. 1999, A&A 347, 739
Reinecke, M., Hillebrandt, W. & Niemeyer, J.-C. 2002, A&A 386, 936
Reinecke, M., Hillebrandt, W. & Niemeyer, J.-C. 2002, A&A 391, 1167
Sorokina, E. & Blinnikov, S. 2002, Proc. ESO/MPA/MPE Workshop on "The Physics of Supernovae", Garching, W. Hillebrandt and B. Leibundgut (Eds.). Springer, in print